ISSN 1066-3622, Radiochemistry, 2019, Vol. 61, No. 5, pp. 632–636. © Pleiades Publishing, Inc., 2019.
Russian Text © The Author(s), 2019, published in Radiokhimiya, 2019, Vol. 61, No. 5, pp. 446–449.

Specific Features of the ^{226}Ra, ^{238}U, and ^{232}Th Distribution in the Surface Layer of Marine Sediments under the Conditions of Active Biosedimentation in the Arctic Front Zone

M. M. Domanov*[a], A. K. Abrosimov[a], and E. A. Novichkova[a]

Shirshov Institute of Oceanology, Russian Academy of Sciences, Nakhimovskii pr. 36, Moscow, 117997 Russia
**e-mail domanov@ocean.ru*

Received October 17, 2018; revised October 17, 2018; accepted December 25, 2018

Abstract—The distribution of natural radionuclides and organic matter in bottom sediments of the active biosedimentation zone on the section drawn through the arctic front of the North Atlantic was studied. The ratios of the amounts of ^{226}Ra, ^{238}U, and ^{232}Th, both deposited in the surface layer of bottom sediments from seawater and supplied with the terrigenic material, were estimated. Direct deposition of radium from water to marine sediments correlates with the organic matter content. The concentration of radium that is not in equilibrium with uranium varies in the range 95–99% of the total content and increases with an increase in the content of chloroform-soluble bitominoid (CB) (R = 0.95). The deposition of nonequilibrium ^{238}U from water to bottom deposits is also significant and ranges from 42 to 69% of the total ^{238}U content. The concentration ratio of nonequilibrium uranium and nonequilibrium radium in the sediments decreases with increasing depth and increases with an increase in the CB content of the deposit. Positive correlation is observed between the content of thorium and total uranium (R = 0.93) and of its nonequilibrium and terrigenic fractions (R = 0.93 and 0.94, respectively).

Keywords: sediment, hydrocarbons, radionuclides

DOI: 10.1134/S1066362219050187

Based on data on spatial distribution of ^{226}Ra, ^{238}U, and ^{232}Th in the surface layer of marine sediments [1–6], various hypotheses concerning the sources and accumulation mechanism of natural radionuclides in the marine sediments were suggested [3, 5]. In so doing, the possibility of direct deposition of ^{226}Ra from seawater was underestimated or rejected at all [3]. On the contrary, as shown in [4, 5], direct transfer of radium from water to marine sediments is a significant factor of its accumulation in the surface layer of bottom sediments. Such mechanism of radionuclide deposition is the most pronounced in active biosedimentation zones, but studies of this process are scarce. It is also known that there is positive correlation between the content of ^{226}Ra and ^{232}Th and the content of aromatic organic substances, favoring selective accumulation of radionuclides, in the sediment [7]. The relationships of the ^{226}Ra and ^{232}Th distribution in the surface layer of the sediments and correlation of these radionuclides with the organic matter of the sediments reflect the regional features of the bottom sediment formation.

In this work, with the aim of determining the conditions of formation of zones with increased concentrations of ^{226}Ra, ^{238}U, and ^{232}Th in bottom sediments with high content of organic matter, we studied the distribution of natural radionuclides and organic matter in bottom sediments of the active biosedimentation zone on the section drawn through the arctic front of the North Atlantic. We estimated the ratios of the ^{226}Ra, ^{238}U, and ^{232}Th, both deposited in the surface layer of bottom sediments from seawater and supplied with the terrigenic material.

SAMPLING REGION AND PROCEDURE

The latitude section along 60°N crosses the steady-state polar front with sharply changing hydrological, hydrochemical, and biological characteristics of the medium. In this highly productive zone of the ocean, the annual average production varies within the front from 200 to 500 $mg_C\ m^{-2}$ daily [8]. Mass growth of coccolithophores is observed every year in this region;

Table 1. Coordinates of stations in the area studied and sediment characteristics (0–5 cm horizon)

Station no.	Latitude (N)	Longitude (W)	Depth, m	Sediment type
3348	59°30′	18°	2183	Gray, fine alevrite, gravel impurity
3352	59°30.1′	20°38.47′	2821	Brown pelite with fine alevrite impurity
3545	59°29.91′	20°41.68′	2825	Brown sand with pelite impurity, foraminifer
3359	59°30′	24°40.56′	2515	Dark brown pelite
3556	59°30.31′	24°42.96′	2517	Dark gray-brown alevrite–pelite foraminifer silt
3568	59°30′	28°39.97′	1694	Olive-brown sand–pelite foraminifer silt
3378	59°30.12′	32°50.66′	2175	Light brown fine alevrite
3383	59°29′	36°06.15′	3083	Brown fine alevrite
3414	59°58′	43°04.9′	2985	Light brown alevrite with sand impurity

their primary production often amounts to 5–40% of the primary production of phytoplankton [8, 9]. Coccolithophores having calcium skeleton extract calcium from seawater and make the major contribution to the sedimentation flow of calcium carbonate to bottom sediments [10, 11]. Under these conditions, the biological factor is one of the prevalent factors in creation of the sedimentation flow, distribution of the organic matter, and formation of the elemental composition of bottom sediments.

Samples were taken with a Okean-0.25 bottom grab from the surface (0–5 cm) layer of the bottom sediments in the North Atlantic along the 60°N latitude section in the 49th and 51st voyages of Akademik Ioffe research vessel within the framework of the Russian Science Foundation project "World Ocean in the XXI Century: Climate, Ecosystems, Resources, Catastrophes" [12, 13]. The station locations and sediment characteristics are given in Table 1. The surface layer is mainly constituted by coccolith and foraminifer lime sand of various particle sizes. The distribution of *Neogloboquadrina pachyderma (s)* (Ehrenberg) polar plankton foraminifera species, IRD (ice rafted debris), and $CaCO_3$ in the sediments suggests the interglacial (Holocene) conditions of sediment accumulation in this region [14].

The ^{226}Ra and ^{232}Th concentrations in the sediments were determined at the Laboratory of Dosimetry and Environmental Radioactivity, Department of Chemistry, Moscow State University using a γ-ray spectrometer equipped with a GC-3020 high-purity Ge detector with the 30% efficiency on the ^{60}Co line (1.332 MeV) and resolution of 1.8 keV at this energy. GENIE-400 PC software was used. ^{226}Ra was determined by its daughter product, ^{214}Bi (energy 609 keV), and ^{232}Th, by ^{228}Ac (energies 583 and 909 keV). Prior to measurements, the sediments packed in sealed containers were kept for a month to accumulate the decay daughter products. The determination accuracy was 4–7% for ^{226}Ra and 7–12% for ^{232}Th.

In addition, we measured the content of Al and U in the sediments by inductively coupled plasma mass spectrometry (ICP MS). GSD-2 and SDO-1 standard samples were used for the quality control. The measurement error was 5% for Al and 13% for U.

The content of chloroform-soluble bituminoid (CB) in the sediments was determined by cold extraction on an ultrasonic bath. The samples preliminarily dried at 60°C were extracted three times with chloroform, and the extracts were combined and evaporated on a rotary evaporator.

RESULTS AND DISCUSSION

The results of determining the ^{226}Ra, ^{238}U, ^{232}Th, Al, and CB concentrations are given in Table 2. The ^{226}Ra, ^{232}Th, and ^{238}U concentrations in the surface layer of the sediments were compared to the organic matter (CB) content of the sediment (Fig. 1).

The most significant changes in the ^{226}Ra and organic matter (CB) concentrations in the sediments were observed in the eastern part of the section (20–30°W, Iceland Basin). This part of the section is located in the region of arctic front in the highly productive zone of the ocean. The correlation of the ^{226}Ra concentration with the organic matter content of the sediment is well pronounced (correlation coefficient R = 0.95), suggesting significant contribution of the biological community to the ^{226}Ra accumulation in bottom sediments of increased productivity (Fig. 2).

The ^{226}Ra concentration in the sediment is deter-

Table 2. Concentrations of ^{226}Ra, ^{238}U, ^{232}Th, Al, and CB in the surface layer of sediments

Station no.	^{226}Ra, Bq kg^{-1}	^{238}U, Bq kg^{-1}	^{232}Th, Bq kg^{-1}	Al, %	CB, mg g^{-1}	Depth, m
3348	75.1	5	6.9	2.1	0.016	2183
3352	43.1	5.8	4.4	2.2	0.013	2821
3545	36.3	4.6	4.1	1.9	0.012	2825
3359	67.3	8.5	10.5	3.5	0.019	2515
3556	69.9	5.9	7.2	2.4	0.0185	2517
3568	67.4	5.8	5.9	2.3	0.0175	1694
3378	28.5	4.9	5.2	2	0.01	2175
3383	19.1	7.6	10.7	3	0.01	3083
3414	26.5	8.9	12.2	3	0.01	2985

mined by the sum of the concentrations of ^{226}Ra incorporated in biogenic particles such as carbonates, opal, organic matter, ^{226}Ra equilibrium with uranium, ^{226}Ra supplied to the sediment with the terrigenic material in

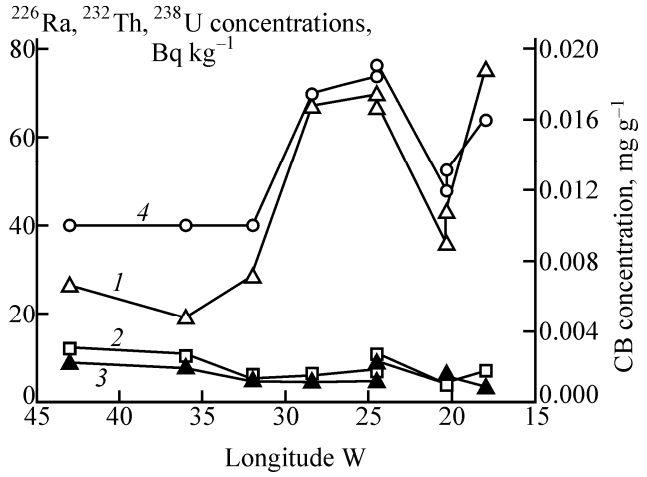

Fig. 1. Concentrations of (*1*) ^{226}Ra, (*2*) ^{232}Th, (*3*) ^{238}U, and (*4*) CB on the section.

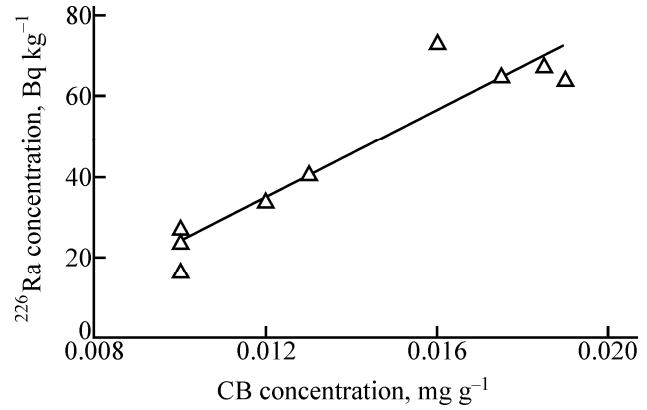

Fig. 2. Correlation between the ^{226}Ra concentration in the sediment and the chloroform-soluble bitominoid content.

which it occurs in radioactive equilibrium in the series ^{238}U–^{230}Th–^{226}Ra, and ^{226}Ra produced by the ^{230}Th decay. By subtracting from the total radium activity ($^{226}Ra_{tot}$) the concentration of radium in equilibrium with terrigenic uranium ($^{226}Ra_{eq}$), we can estimate the radium excess, i.e., the amount of nonequilibrium radium ($^{226}Ra_{exc}$) directly extracted from water and produced by the decay of ^{230}Th ($^{226}Ra_{Io}$). The nonequilibrium radium content varies in the range 95–99% and increases with an increase in the CB content of the sediment (R = 0.95). The content of radium produced by the ^{230}Th decay was not calculated in this study. However, for indirect estimation of $^{226}Ra_{Io}$ at station 3348, we can use the data of Kuznetsov et al. [5], according to which the $^{226}Ra_{Io}/^{226}Ra_{tot}$ ratio in ocean sediments varied in the range 0.2–0.9 (mean 0.46) and depended on the sediment accumulation rate (R = –0.77). The corresponding regression equation has the form

$$y = -0.1539x + 0.7893,$$

where $y = {}^{226}Ra_{Io}/^{226}Ra_{tot}$, and x is the sediment accumulation rate, cm/1000 years.

According to the data given in [16], the sediment accumulation rate in the region of station 3348 is 1 cm/2000 years. The $^{226}Ra_{Io}/^{226}Ra_{tot}$ ratio thus obtained is 0.71. Thus, the relative amount of ^{226}Ra extracted from water can be estimated at 29%.

Several factors determining both the intensity of the Ra supply to the sediments and the ratio of the dissolved and suspended Ra vary with the depth. This is associated both with a decrease in the organic matter content of the sediments and with the Ra release into the aqueous phase upon organic matter decomposition. A decrease in the total ^{226}Ra content and in the radium excess in the suspended material with the depth was noted previously for suspended material samples from

Table 3. Concentrations of nonequilibrium ^{226}Ra (excess, $^{226}Ra_{exc}$) and of terrigenic uranium fraction ($^{238}U_{ter}$) and uranium excess ($^{238}U_{exc}$) in the surface layer of sediments

Station no.	$^{226}Ra_{exc}$, Bq kg^{-1}	$^{238}U_{ter}$, Bq kg^{-1}	$^{238}U_{exc}$, Bq kg^{-1}	$^{238}U/^{226}Ra$, %	Depth, m
3348	74.4	0.70	4.3	6.7	2183
3352	42.4	0.73	5.0	13.3	2821
3545	35.7	0.62	4.0	12.7	2825
3359	66.2	1.13	7.4	12.6	2515
3556	69.1	0.79	5.1	8.4	2517
3568	66.7	0.75	5.0	8.5	1694
3378	27.8	0.66	4.2	17.1	2175
3383	18.1	0.98	6.6	39.9	3083
3414	25.4	1.14	7.7	33.5	2985

sedimentation traps [17]. In the depth range 389–5086 m, the ^{226}Ra concentration in the suspended material decreased by a factor of 2.2 and the flow of excess ^{226}Ra, by a factor of 5.2 (PARFLUX E site) [17]. Degradation of the organic matter continues in the sediment. In the process, the $^{226}Ra_{Io}$ produced by the ^{230}Th decay is accumulated in the sediment. Thus, various processes differing in the direction and intensity make up a complex system of the formation of the radionuclide concentration pattern at different depths. In the region studied, the total Ra content and its nonequilibrium fraction (^{226}Ra excess) in the sediments decrease with increasing depth (R = –0.82) for the majority of samples except station 3378.

The ^{238}U concentration in the sediment varies in the range 4.6–8.9 Bq kg^{-1}. The mean value is 6.3 Bq kg^{-1} (Tables 2, 3). This value is close to the ^{238}U clarke in basalt (7.5 Bq kg^{-1}) [18]. Because the U : Al clarke ratio adequately reflects their content in terrigenic sediments, the terrigenic fraction of ^{238}U ($^{238}U_{ter}$) in the sediment can be estimated as

$$^{238}U_{ter} = (^{238}U_{cl}/Al_{cl})Al_{meas},$$

where $^{238}U_{cl}/Al_{cl}$ is the ^{238}U to Al clarke ratio in basalts and Al_{meas} is the aluminum concentration in the sample.

The terrigenic fraction of ^{238}U in the sediment is 13–14%. The uranium excess ($^{238}U_{exc}$, a part of ^{238}U bonded with biogenic particles such as carbonates, opal, organic matter) was determined by subtracting the terrigenic fraction from the total ^{238}U content of the sediment (Table 3). This fraction of ^{238}U has probably been extracted directly from seawater and is not associated with the daughter isotopes. Similar conclusion was made previously in [17]. The uranium excess is 86–87% of the total ^{238}U content of the sediments. These results confirm the conclusion [4] that the major fraction of uranium at deep ocean stations originates from seawater uranium.

Table 4 illustrates the correlation between CB, ^{226}Ra, ^{232}Th, and ^{238}U and their fractions in the sediments.

The ^{232}Th concentration (Bq kg^{-1}) varies from 4.1 to 12.2 at a mean value of 6.2. Increased ^{232}Th content is characteristic of the western part of the section, in which alevrite and sand fractions with an impurity of gravel materials prevail. These results agree with the conclusions made in [5] that the Th concentration in the sediments is determined by the supply of the terrigenic material in which Th is present in the crystal lattice of the minerals. The ^{232}Th concentration correlates with the Al concentration (R = 0.94). Positive correlation is observed between the content of Th and U (R = 0.93) and of its biogenic and terrigenic fractions (R = 0.93 and 0.94, respectively). In the zone with increased bituminoid concentration, no increase in the Th and U concentrations in the sediment was noted. Positive correlation is observed between the $^{226}Ra/^{232}Th$ activity ratio and the CB concentration in the sediment, which is due to an increase in the ^{226}Ra concentration and a decrease in the ^{232}Th concentration

Table 4. Correlation matrix of the correlation coefficients

Parameter	^{226}Ra	^{232}Th	^{238}U	$^{238}U_{exc}$	$^{238}U_{ter}$	$^{226}Ra_{exc}$	CB
^{226}Ra	1.00					1.00	0.95
^{232}Th		1.00	0.93	0.93	0.94		
^{238}U		0.93	1.00	1.00	1.00		
$^{238}U_{exc}$		0.93	1.00	1.00			
$^{238}U_{ter}$		0.94	1.00		1.00		
$^{226}Ra_{exc}$	1.00					1.00	0.95
CB	0.95					0.95	1.00

in the sediment with an increase in the CB content.

Thus, we have confirmed the hypothesis that direct deposition of Ra from seawater is a significant factor of the Ra accumulation in the surface layer of bottom sediments. The radium adsorbed from water and produced by the decay of the parent ^{230}Th makes up the major fraction of radium in the sediment (95–99%). The fraction of terrigenic (equilibrium with uranium) radium is insignificant. The content of the nonequilibrium Ra in the sediments increases with the CB content of the sediments (R = 0.95). Indirect estimation of the fraction of Ra produced by the ^{230}Th decay (station 3348) gives the value of 71% of the total Ra content. The content of nonequilibrium ^{238}U deposited from water is 86–87% of the total ^{238}U content of the sediments. The U/Ra concentration ratio in the sediments increases with the depth and decreases with an increase in the CB content of the sediment. Positive correlation is observed between the content of Th and U (R = 0.93) and of its nonequilibrium and terrigenic fractions (R = 0.92 and 0.94, respectively).

FUNDING

The study was financially supported by the Russian Science Foundation (project no. 14-50-00095). The data were processed in part within the framework of the government assignment, theme no. 0149-2019-0007.

ACKNOWLEDGMENTS

The authors are grateful to Acad. A.P. Lisitsyn for the general guidance and to participants of the expedition for the assistance in sampling.

CONFLICT OF INTEREST

The authors declare that they have no conflict of interest.

REFERENCES

1. Piggot, C.S., *Am. J. Sci*., 1933, vol. 25, no. 5, pp. 229–338.
2. Rona, E. and Urry, F.D., *Am. J. Sci*., 1952, vol. 250, pp. 241–245.
3. *Nuclear Geology*, Faul, H., Ed., New York: Wiley, 1954.
4. Starik, I.E., Kuznetsov, Yu.V., and Legin, V.K., *Radiokhimiya*, 1959, vol. 1, no. 3, pp. 321–324.
5. Kuznetsov, Yu.V., Simonyak, Z.V., Lisitsin, A.P., and Frenklikh, M.S., *Geokhimiya*, 1968, no. 3, pp. 323–333.
6. Miyake, Y., Saruhashi, K., and Sugimura, Y., *Rec. Oceanogr. Works Jpn., New Ser*., 1968, vol. 9, no. 2, pp. 179–187.
7. Domanov, M.M., Verkhovskaya, Z.I., and Domanova, E.G., *Petrol. Chem.*, 2011, vol. 51, no. 4, pp. 257–263.
8. Koblents-Mishke, O.I., *Biologiya okeana* (Ocean Biology), Moscow: Nauka, 1977, vol. 1, pp. 62–64.
9. Poulton, A.J., Adey, T.R., Balch, W.M., and Holligan, P.M., *Deep Sea Res. Part II*, 2007, vol. 54, pp. 538–557.
10. Poulton, A.J., Painter, S.C., Young, J.R., et al., *Global Biogeochem. Cycles*, 2013, vol. 27, pp. 1023–1033.
11. Milliman, J.D., *Global Biogeochem. Cycles*, 1993, vol. 7, no. 4, pp. 927–957.
12. Klyuvitkin, A.A., Politova, N.V., Novigatsky, A.N., et al., *Oceanology*, 2016, vol. 56, no. 5, pp. 760–762.
13. Klyuvitkin, A.A., Politova, N.V., Novigatsky, A.N., et al., *Oceanology*, 2017, vol. 57, no. 3, p. 465.
14. Broecker, W. and Clark, E., *Paleoceanogr. Paleoclimatol*., 2009, vol. 24, paper PA3205. http://dx.doi.org/10.1029/2009PA001731.
15. Nikolaeva, D.Yu., Bashirova, L.D., Novichkova, E.A., and Kozina, N.V., *Obshch. Sreda. Razv.*, 2017, no. 4, pp. 145–151.
16. Klyuvitkin, A.A., Novigatsky, A.N., and Politova, N.V., in *Geologiya morei i okeanov: Materialy XXII Mezhdunarodnoi nauchnoi konferentsii (Shkoly) po morskoi geologii* (Geology of Seas and Oceans: Proc. XXII Int. Scientific Conf. (School) on Marine Geology), Moscow: Inst. of Oceanology, Russ. Acad. Sci., 2017, vol. III, pp. 82–86.
17. Brewer, P.G., Nozaki, Y., Spencer, D.W., and Fleer, A.P., *J. Marine Res*., 1980, vol. 38, no. 4, pp. 703–728.
18. Taylor, S.R., *Geochim. Cosmochim. Acta*, 1964, vol. 28, pp. 1273–1285.

Translated by G. Sidorenko